Jets in pp at NNLO

João Pires*
Universita di Milano-Bicocca and
Universita di Genova, INFN sezione di Genova

HP2.5
3-5 September 2014 Florence, Italy

* based on:

"Second order QCD corrections to gluonic jet production at hadron colliders"

J. Currie, A. Gehrmann-De Ridder, T. Gehrmann, N. Glover, JP, S. Wells, arXiv:1407.5558

arXiv:1310.3993 JHEP 1401 (2014) 110, arXiv:1301.7310 Phys.Rev.Lett. 110 (2013) 16

"Perturbative QCD description of jet data from LHC Run-I and Tevatron Run-II"

S.Carrazza, JP, arXiv:1407.7031

Inclusive jet and dijet cross sections

- look at the production of jets of hadrons with large transverse energy in
  - inclusive jet events $pp \to j + X$
  - exclusive dijet events $pp \to 2j$
- cross sections measured as a function of the jet p_T, rapidity y and dijet invariant mass m_{jj} in double differential form

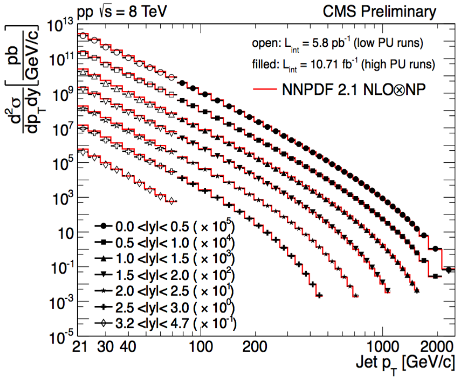

(CMS-PAS-SMP-12-012)

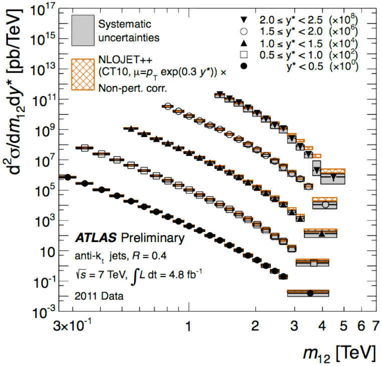

(ATLAS-CONF-2012-021)

Inclusive jet cross section

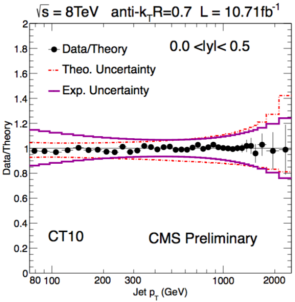

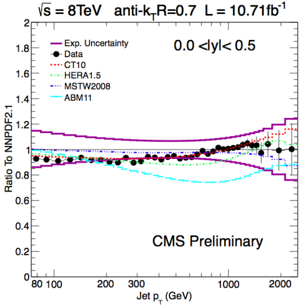

<u>Motivation for NNLO</u>

- experimental uncertainties at high-p_T smaller than theoretical $\rightarrow$ need pQCD predictions to NNLO accuracy

Inclusive jet cross section

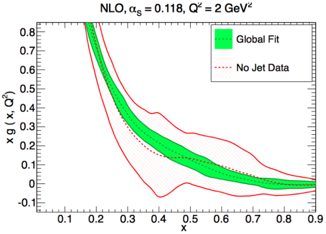

NNPDF collaboration

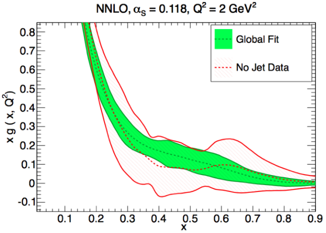

NNPDF collaboration

Motivation for NNLO

- experimental uncertainties at high-p_T smaller than theoretical $\rightarrow$ need pQCD predictions to NNLO accuracy
- collider jet data can be used to constrain parton distribution functions
- size of NNLO correction important for precise determination of PDF's
- inclusion of jet data in NNLO parton distribution fits requires NNLO corrections to jet cross sections

Inclusive jet cross section

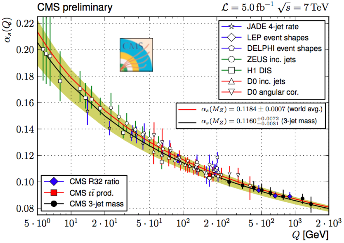

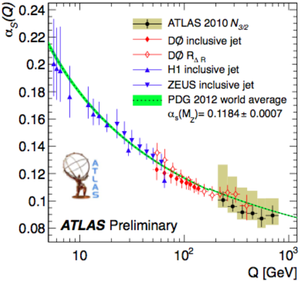

Motivation for NNLO

- experimental uncertainties at high-p_T smaller than theoretical $\rightarrow$ need pQCD predictions to NNLO accuracy
- collider jet data can be used to constrain parton distribution functions
- size of NNLO correction important for precise determination of PDF's
- inclusion of jet data in NNLO parton distribution fits requires NNLO corrections to jet cross sections
- α_s determination from hadronic jet observables limited by theoretical uncertainty due to scale choice

inclusive jet and dijet cross sections

State of the art:

- dijet production is completely known in NLO QCD [Ellis, Kunszt, Soper '92], [Giele, Glover, Kosower '94], [Nagy '02]
- NLO+Parton shower [Alioli, Hamilton, Nason, Oleari, Re '11]
- NLO EW corrections [Dittmaier, Huss, Speckner '12]
- approximate NNLO threshold corrections [Kidonakis, Owens '00], [Florian, Hinderer, Mukherjee, Ringer, Vogelsang '13]

Goal:

- obtain the jet cross sections at NNLO exact accuracy in double differential form

$$\frac{\mathrm{d}^2\sigma}{\mathrm{d}p_T\mathrm{d}|y|} \qquad \frac{\mathrm{d}^2\sigma}{\mathrm{d}m_{jj}\mathrm{d}y^*}$$

$pp \to 2j$ at NNLO: gluonic contributions

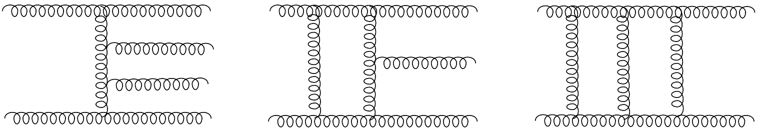

$A_6^{(0)}(gg \to gggg)$ $A_5^{(1)}(gg \to ggg)$ $A_4^{(2)}(gg \to gg)$

[Berends, Giele '87], [Mangano, Parke, Xu '87], [Britto, Cachazo, Feng '06]
[Bern, Dixon, Kosower '93]
[Anastasiou, Glover, Oleari, Tejeda-Yeomans '01],[Bern, De Freitas, Dixon '02]

$$\mathrm{d}\hat{\sigma}_{NNLO} = \int_{\mathrm{d}\Phi_4} \mathrm{d}\hat{\sigma}_{NNLO}^{RR} + \int_{\mathrm{d}\Phi_3} \mathrm{d}\hat{\sigma}_{NNLO}^{RV} + \int_{\mathrm{d}\Phi_2} \mathrm{d}\hat{\sigma}_{NNLO}^{VV}$$

- explicit infrared poles from loop integrations
- implicit poles in phase space regions for single and double unresolved gluon emission
- procedure to extract the infrared singularities and assemble all the parts in a parton-level generator
- differential cross sections$\to$ kinematics of the final state intact to apply arbitrary phase space observable cuts

NNLO antenna subtraction

$$
\begin{aligned}
\mathrm{d}\hat\sigma_{NNLO} &= \int_{\mathrm{d}\Phi_4}\left(\mathrm{d}\hat\sigma^{RR}_{NNLO}-\mathrm{d}\hat\sigma^{S}_{NNLO}\right)\\
&+ \int_{\mathrm{d}\Phi_3}\left(\mathrm{d}\hat\sigma^{RV}_{NNLO}-\mathrm{d}\hat\sigma^{T}_{NNLO}\right)\\
&+ \int_{\mathrm{d}\Phi_2}\left(\mathrm{d}\hat\sigma^{VV}_{NNLO}-\mathrm{d}\hat\sigma^{U}_{NNLO}\right)
\end{aligned}
$$

- $\mathrm{d}\hat\sigma^{S}_{NNLO}$: real radiation subtraction term for $\mathrm{d}\hat\sigma^{RR}_{NNLO}$
- $\mathrm{d}\hat\sigma^{T}_{NNLO}$: one-loop virtual subtraction term for $\mathrm{d}\hat\sigma^{RV}_{NNLO}$
- $\mathrm{d}\hat\sigma^{U}_{NNLO}$: two-loop virtual subtraction term for $\mathrm{d}\hat\sigma^{VV}_{NNLO}$
- subtraction terms constructed using the antenna subtraction method at NNLO for hadron colliders $\rightarrow$ presence of initial state partons to take into account
- contribution in each of the round brackets is finite, well behaved in the infrared singular regions and can be evaluated numerically

NNLO antenna subtraction

- universal factorisation of both colour ordered matrix elements and the $(m+2)$- particle phase space $\rightarrow$ colour connected unresolved particles

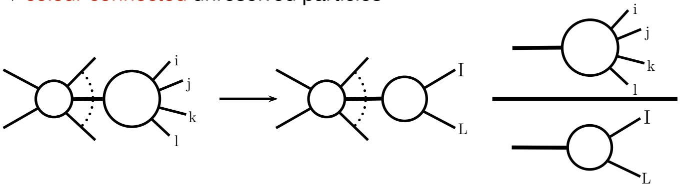

$$|M_{m+4}(\ldots,i,j,k,l,\ldots)|^2 \; J(\{p_{m+4}\}) \;\longrightarrow |M_{m+2}(\ldots,I,L,\ldots)|^2 \; J(\{p_{m+2}\}) \;\cdot X_4^0(i,j,k,l)$$

- momentum map $\{p_i,p_j,p_k,p_l\} \rightarrow \{p_I,p_L\}$ enforces momentum conservation away from the unresolved limits
- phase-space factorisation

$$\begin{aligned} \mathrm{d}\Phi_{m+2}(p_a,\ldots,p_i,p_j,p_k,p_l,\ldots,p_{m+2}) \quad &= \quad \mathrm{d}\Phi_m(p_a,\ldots,p_I,p_L,\ldots,p_{m+2}) \\ &\quad\;\; \mathrm{d}\Phi_{X_{ijkl}}(p_i,p_j,p_k,p_l) \end{aligned}$$

- integrated antennae is the inclusive integral

$$\mathcal{X}^0_{ijkl}(s_{ijkl}) = \frac{1}{C(\epsilon)^2}\int \mathrm{d}\Phi_{X_{ijkl}}(p_i,p_j,p_k,p_l)X_4^0(i,j,k,l)$$

NNLO antenna subtraction

Implementation checks $pp \to 2j$ at NNLO:

- subtraction terms correctly approximate the matrix elements in all unresolved configurations of partons j, k

$$\boxed{\mathrm{d}\hat{\sigma}^{RR,RV}_{NNLO} \xrightarrow{\forall\{j,k\},\{j\}\to 0} \mathrm{d}\hat{\sigma}^{S,T}_{NNLO}}$$

- local (pointwise) analytic cancellation of all infrared explicit ϵ-poles when integrated subtraction terms are combined with one, two-loop matrix elements

$$\boxed{\mathcal{P}oles\left(\mathrm{d}\hat{\sigma}^{RV}_{NNLO} - \mathrm{d}\hat{\sigma}^{T}_{NNLO}\right) = 0}$$

$$\boxed{\mathcal{P}oles\left(\mathrm{d}\hat{\sigma}^{VV}_{NNLO} - \mathrm{d}\hat{\sigma}^{U}_{NNLO}\right) = 0}$$

- leading and subleading colour
- process independent NNLO subtraction scheme
- allows the computation of multiple differential distributions in a single program run

Jet production partonic channels

Fraction of jets per initial state contribution

LHC

- $gg \to gg$ dominates at low p_T
- $qg \to qg$ important in all p_T regions
- $qq \to qq$ dominant at high p_T

Tevatron

- qg and $q\bar{q}$ dominant

Present results at NNLO for

- $gg \to gg$ at leading colour
- $gg \to gg$ at subleading colour
- $q\bar{q} \to gg$ at leading colour

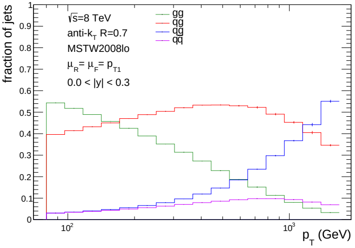

(LHC 8 TeV)

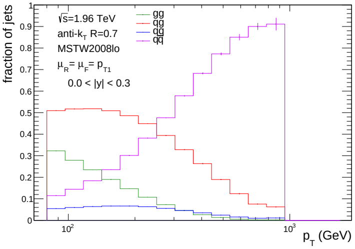

(Tevatron 1.96 TeV)

Numerical setup

(J.Currie, A. Gehrmann-De Ridder, T.Gehrmann, N. Glover, JP '13)

- pp collisions at $\sqrt{s} = 8$ TeV
- jets identified with the anti-k_T jet algorithm with resolution parameter $R = 0.7$
- jets accepted at rapidities $|y| < 4.4$
- leading jet with transverse momentum $p_T > 80$ GeV
- subsequent jets required to have at least $p_T > 60$ GeV
- MSTW2008nnlo PDF for all fixed-order predictions
- dynamical factorization and renormalization scales equal to the leading jet p_T ($\mu_R = \mu_F = \mu = p_{T1}$)
- present results for full colour $gg \to gg$ scattering and $q\bar{q} \to gg$ leading colour combined at NNLO

Inclusive jet p_T distribution at NNLO

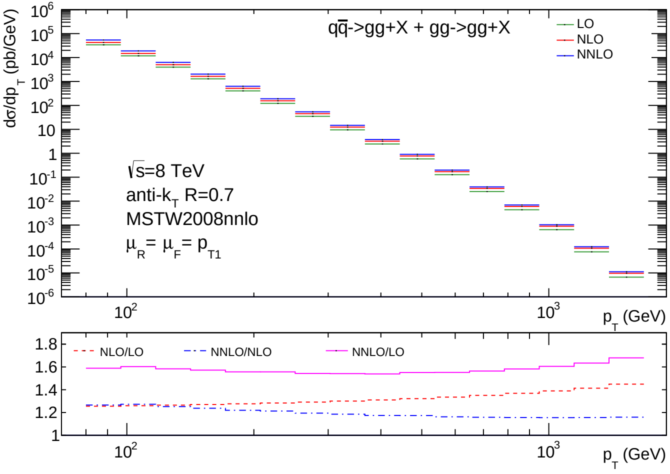

- all jets in an event are binned
- NNLO correction stabilizes the NLO k-factor growth with p_T
- NNLO corrections $15 - 26\%$ with respect to NLO

Double differential inclusive jet p_T distribution at NNLO

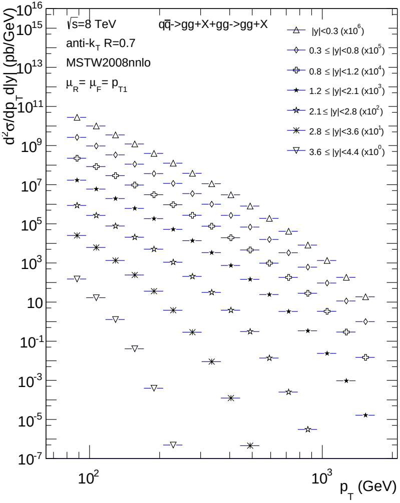

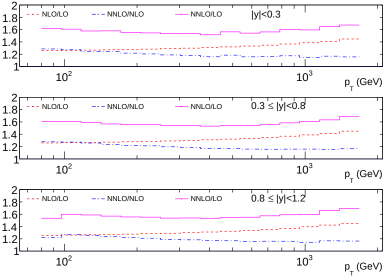

double differential k-factors

- NNLO prediction increases between 25% to 15% with respect to the NLO cross section
- similar behaviour between the rapidity slices

Double differential exclusive dijet mass distribution at NNLO

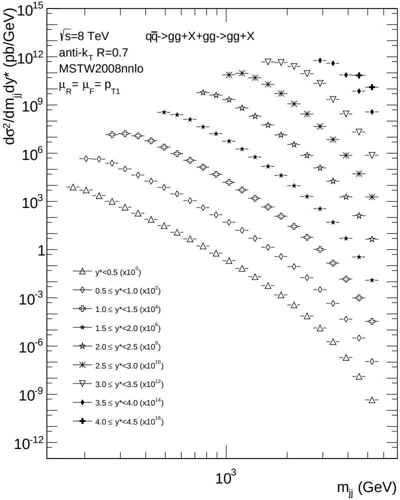

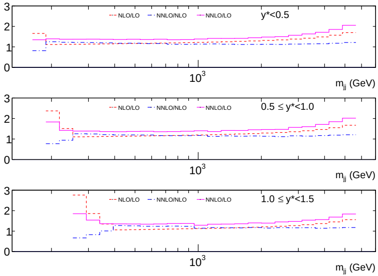

double differential k-factors

- NNLO corrections up to 20% with respect to the NLO cross section
- similar behaviour between the $y^* = 1/2|y_1 - y_2|$ slices

Inclusive jet p_T scale dependence $(gg \to gg + X)$

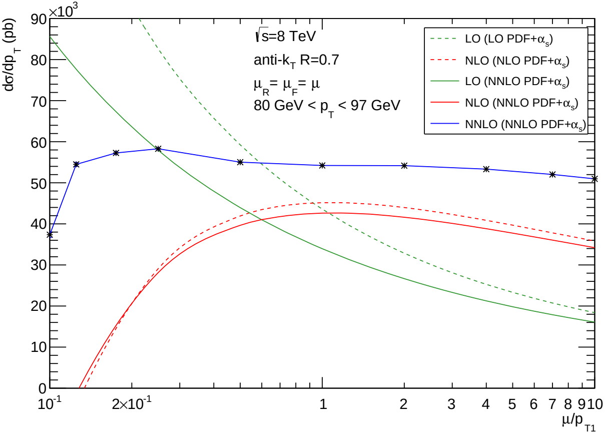

- scale dependence study gluons only $N_F = 0$ channel at leading colour
- dynamical scale choice: leading jet p_{T1}
- flat scale dependence at NNLO

Threshold resummation approximation to exact NNLO

- Approximate NNLO results from an improved threshold calculation for the single jet inclusive production [de Florian, Hinderer, Mukherjee, Ringer, Vogelsang '13]
  - $pp \to j + X$ with the threshold limit given by $s_4 = P_X^2 \to 0$
  - near threshold phase space available for real-gluon emission is limited
  - higher kth order coefficient functions dominated by large logarithmic corrections

$$\alpha_s^k w_{ab}^{(k)} \to \alpha_s^k \left(\frac{\log^m(z)}{z} \right)_+ , \qquad m \leq 2k-1, \qquad z = \frac{s_4}{s}$$

  - $\delta(z)$ ✗, 4th tower ✗, $\mathcal{O}$(z) ✗

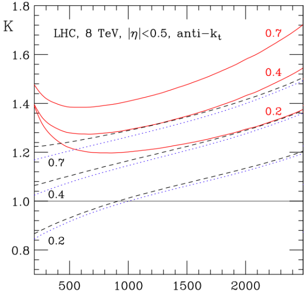

(all-channels)

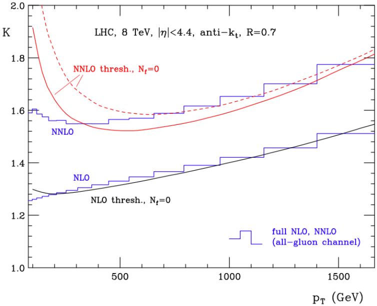

(gluons only channel) - rapidity integrated

NNLO benchmark predictions for jet production

S. Carrazza, JP, arXiv:1407.7031

- understand and characterise the validity of the NNLO threshold approximation by comparing it with the exact computation using the gg-channel
- $\mu_R = \mu_F = p_T$ for both predictions
- comparison performed differential in p_T and rapidity following the exact experimental setups
- NNPDF23_nnlo_as_0118 set for all fixed order predictions
- NLO benchmark curves
  - green dashed curves $\rightarrow$ NLO-threshold gg-channel
  - black dashed curves $\rightarrow$ NLO-exact gg-channel
  - blue dashed curves $\rightarrow$ NLO-exact all channels
- NNLO benchmark curves
  - pink long-dashed curves $\rightarrow$ NNLO-threshold gg-channel $\rightarrow$ $\boxed{\mathrm{d}\sigma^{\mathrm{thresh}}_{gg,NNLO}/\mathrm{d}\sigma_{gg,LO}}$
  - black long-dashed curves $\rightarrow$ NNLO-exact gg-channel $\rightarrow$ $\boxed{\mathrm{d}\sigma^{\mathrm{exact}}_{gg,NNLO}/\mathrm{d}\sigma_{gg,LO}}$

Tevatron CDF Run-II $\sqrt{s}$=1.96 TeV

S. Carrazza, JP, arXiv:1407.7031

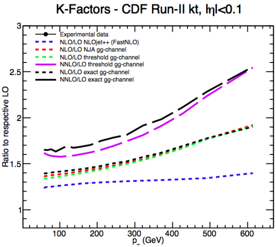

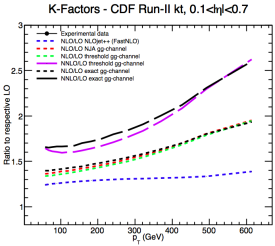

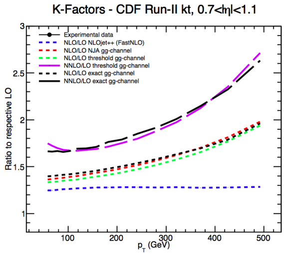

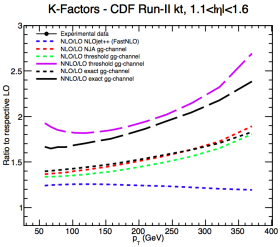

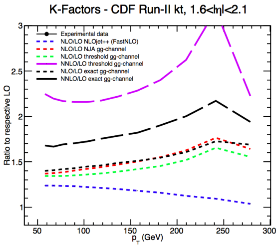

- differences $\leq$ 15% at low-p_T in the central regions
- in the forward region differences $\geq$40% for all p_T regions

LHC ATLAS 2010 $\sqrt{s}$=7 TeV

S. Carrazza, JP, arXiv:1407.7031

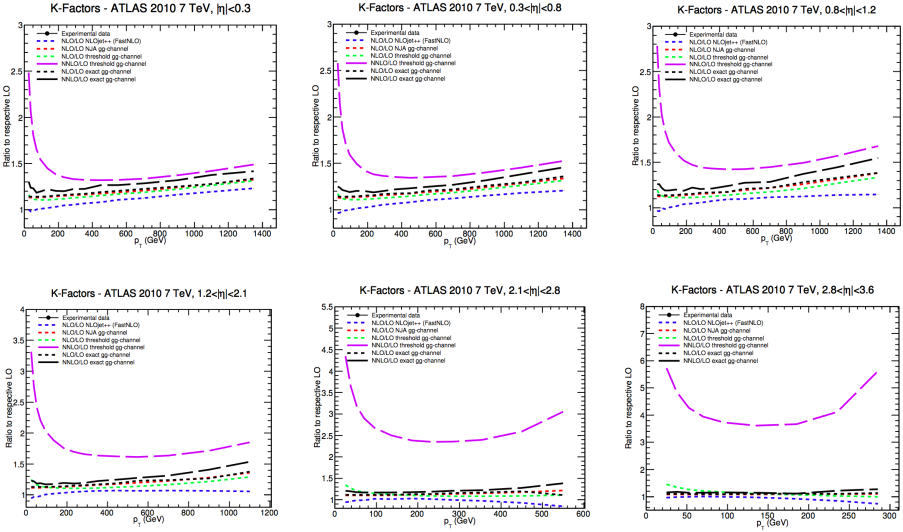

- differences large at small p_T and increase with rapidity
- exact NNLO k-factor decreases with rapidity, NNLO threshold k-factor increases with rapidity

Conclusions

- antenna subtraction method generalised for the calculation of NNLO QCD corrections for exclusive collider observables with partons in the initial-state
- explicit ϵ-poles in the matrix elements are analytically cancelled by the ϵ-poles in the subtraction terms
- non-trivial check of analytic cancellation of infrared singularities between double-real, real-virtual and double-virtual corrections
- successful inclusion of subleading colour contributions at NNLO with the antenna subtraction method
- first exact results for $gg \to gg + X$ and $q\bar{q} \to gg + X$ at NNLO
- perfomed comparison between exact NNLO results and approximate NNLO results from threshold resummation in the gg-channel
  - largest differences arise at low-p_T for central rapidities and all p_T at large rapidities
  - differences are smaller at the Tevatron than at the LHC 7 TeV

Future work:

- include remaining channels involving the quark contributions
  - qg channel - most important at the LHC
  - leading colour N_F pieces
  - qq channel - important at high p_T

Back-up slides

Singly unresolved limits

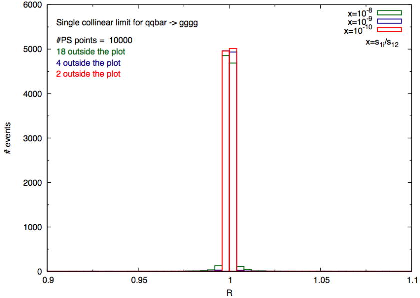

$q \to qg$

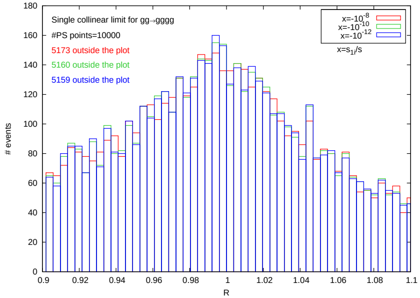

$g \to gg$

Single collinear limits:

- generate phase space points with s_{jk} or s_{1i} small

Distributions with a broader shape due to:

- angular correlations in matrix elements and antenna functions when an initial/final state gluon splits into two gluons not accounted for by the subtraction term $\to$ non-locality of subtraction term

Angular terms subtraction

- angular terms vanish after averaging over the azimuthal angle
- not-relevant for reproducing the correct $1/\epsilon$-poles in virtual contributions

$$\frac{1}{2\pi}\int_0^{2\pi} \mathrm{d}\phi\,(p_l\cdot k_\perp) = 0\,, \qquad \frac{1}{2\pi}\int_0^{2\pi} \mathrm{d}\phi\,(p_l\cdot k_\perp)^2 = -k_\perp^2\,\frac{p\cdot p_l\; n\cdot p_l}{p\cdot n}$$

$$\Theta_{F_3^0}(i,j,z,k_\perp) \sim A\cos(2\phi+\alpha)$$

- combine phase space points related to each other by a rotation of the system of unresolved partons $\{p_i,p_j\} \to \{p'_i,p'_j\}$

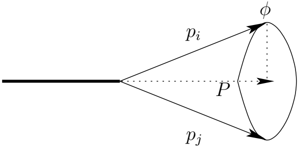

$$p_i^\mu = zp^\mu + k_\perp^\mu - \frac{k_\perp^2}{z}\,\frac{n^\mu}{2p\cdot n}\,, \qquad p_j^\mu = (1-z)p^\mu - k_\perp^\mu - \frac{k_\perp^2}{1-z}\,\frac{n^\mu}{2p\cdot n}\,,$$

with $2p_i\cdot p_j = -\dfrac{k_\perp^2}{z(1-z)}\,,$ $\qquad p^2 = n^2 = k_\perp.p = k_\perp.n = 0$

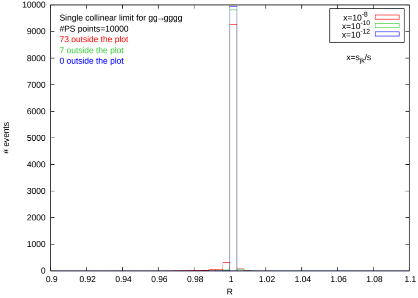

$g \to gg$

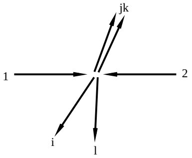

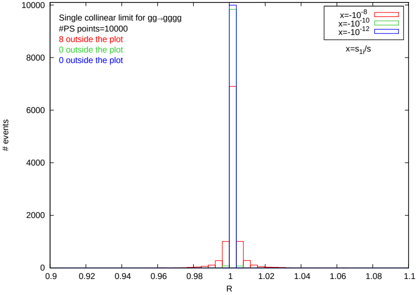

$g \to gg$

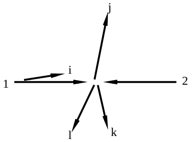

- locality of the subtraction method achieved by combining 2-phase space points
- in both collinear limits combining phase space points largely cancels angular dependent terms
- generalizable to multiple collinear emission
- subtract correlations systematically at the phase space generation level

QCD cross sections at subleading color beyond NLO

(J.Currie, A. Gehrmann-De Ridder, N. Glover, JP '13)

- subleading colour matrix elements have incoherent interferences, gluon scattering

$$|\mathcal{M}_6^0|^2 = g^8 N^4 (N^2-1) \sum_{\sigma \in S_6/Z_6} \left[|A_6^{(0)}(\sigma)|^2 + \frac{2}{N^2} A_6^0(\sigma) \Big(A_6^{\dagger 0}(\sigma') + A_6^{\dagger 0}(\sigma'') + A_6^{\dagger 0}(\sigma''') \Big) \right]$$

- one-loop five parton matrix elements, gluon scattering

$$2\Re\left(\mathcal{M}_5^0 \mathcal{M}_5^{\dagger 1}\right) = g^8 N^4 (N^2-1) \sum_{\sigma \in S_5/Z_5} 2\Re\left[A_5^{\dagger 0}(\sigma) A_5^1(\sigma) + \frac{12}{N^2} A_5^{\dagger 0}(\sigma) A_{5,1}^1(\sigma') \right]$$

- $\sigma', \sigma'', \sigma'''$ have no common neighbouring partons with σ

$$\boxed{\Rightarrow \text{ no single, double or triple collinear singularities at subleading colour } \checkmark}$$

- subtract divergences associated with single and double soft gluons only which at subleading colour map completely to the tree-level single soft gluon current $\to X_3^0$ tree level three parton antenna